

CAPICITANCE-BASED WIRELESS MOISTURE CONTENT SENSORS FOR SANDSTONE

D. Thomson, J. Zhao, G. Mustapha and J. Teetaert

SUMMARY

This paper presents an evaluation of measurement techniques of moisture content (MC) in masonry construction, in particular to building stone. Capacitance sensors with three types of physical configurations were investigated and three moisture measurement techniques were evaluated using Agilent LCR handheld meter, a SMT wireless data logger and a home-made LC resonant sensor with Agilent Impedance Analyzer. The moisture content measurements were carried out through wetting and drying cycles by partially submerging the stones in water and drying them in air. The measured data effectively reflect the moisture content variation in the stones during wetting and drying cycles. The testing results also show a good correlation between the capacitance measured by the LCR meter and the output from the SMT data logger. The testing works demonstrate that the dielectric based moisture content measurement is an effective method to monitor the moisture content inside the building materials and field application is very promising with proper calibration of the instruments to the moisture content.

Acknowledgements

This project is financially supported from Public Works and Government Services Canada (PWGSC) and SMT Research Ltd. and accomplished in ISIS Canada Resource Center, Assistance with this project from Hugues Vogel, Chad Klowak and Charleen Choboter in ISIS Canada Resource Center is highly appreciated.

1. INTRODUCTION

The continuous monitoring of the building structural health is prerequisite to taking effective measures to reduce their structural deterioration and performance degradation. Highly developed modern technologies are being implemented into the traditional civil structures for achieving effective and efficient maintenance, renovation and upgrade of the infrastructures and their functionalities. A wide variety of intelligent structures and sensors have been explored and developed in monitoring various structural health related parameters such as strain, deformation, corrosion, pressure, temperature and moisture [1, 2]. A new discipline, coined as civionics, emerges in combining civil engineering and electronics engineering, it applies smart electronics to monitor the health of the structures and materials (SHM) [3, 4].

Among many considerations regarding the structural health, moisture content (MC) in the building materials (such as stone and concrete) has a great impact on strength and durability of the building structures. Effective measurement of the moisture content can be critical to early diagnosis of moisture-driven degradation of materials and structures. Application of continuous monitoring moisture requires developing effective and smart moisture content sensors, which have very good sensitivity, accuracy, reliability, water resistance and durability. Also, it is important to have moisture sensing devices and instruments with low cost, easy installation and operation. So far, a wide range of moisture sensing devices and instruments have been developed for meeting various in-field moisture measuring requirements however, they all have their own limited capabilities for the applications in the fields [5, 6].

A direct moisture measurement method is weight measurement, called the gravimetric method. This method is destructive and not practically useful for field moisture content monitoring. There are many indirect moisture content measurements, most commonly used are electrical methods [7], which are based on electrical resistance and capacitance measurements. Since water can change electrical conductivity of the building materials such as concrete, stone and wood, measurement of the resistivity is often used to indicate the moisture content in these building materials. Water also can change the dielectric properties of the building materials since it has a much higher relative dielectric constant (about 80) than those building materials (around 1-5). Thus, the dielectric constant of the building materials increases with the moisture content, this gives rise to another approach to measuring the moisture content through measuring the dielectric constant variation induced by water. There are many ways to measure the dielectric constant of the materials; capacitance measurement is a most common method. Besides commonly used impedance measurement techniques, currently there is an attractive interest in developing wireless sensing systems for structural health monitoring since highly advanced microelectronics can provide on-board microprocessors and wireless systems with small size and much less cost [8-11]. One of the wireless sensing techniques is called the passive wireless resonant sensing, it has attracted lots of attention due to its low cost and no need for power. An example is an inductor-capacitor (LC) resonant sensing device, the sensing signal can be transferred through two mutually inductive coils without using wire connection and power for the sensors [7, 8]. The objective of this work is to evaluate capacitive moisture content monitoring techniques by measuring the moisture content (MC) in building stones. The capacitive sensors with different electrode configurations were used to measure the moisture content. A normal impedance measurement instrument like LCR meter, a home-made passive wireless inductance-capacitance (LC) resonant sensor and a capacitive wireless moisture sensor developed by SMT Research were used to measure the moisture content.

2. DIELECTRIC BASED MEASUREMENTS

2.1 Dielectric Complex Permittivity

Dielectric property of materials reflects the dielectric polarization ability in response to an external electric field, it is generally a function of the frequency of the field since the polarization process is not instantaneously response to the field and has a phase difference. The relative complex permittivity can be mathematically represented by the formula: $\epsilon_r(\omega) = \epsilon_r'(\omega) - j\epsilon_r''(\omega)$, where the real part ϵ_r' is called as the 'dielectric constant', the imaginary part ϵ_r'' is referred to as the 'dielectric loss'. The ratio of the dielectric constant to the dielectric loss is defined as loss tangent, which is mathematically expressed as: $Tan\delta = \epsilon_r''(\omega) / \epsilon_r'(\omega)$.

The dielectric constant and loss tangent usually vary with homogeneity and anisotropy properties of the dielectric materials.

There are many measurement techniques to determine dielectric properties of materials [12]. A parallel plate capacitor technique is often used since the electric field between two electrodes is uniform, the complex permittivity of materials can be measured using an ideal capacitor model.

$$C = \epsilon_r \epsilon_0 \frac{A}{d} = \epsilon_r C_0 \quad (1)$$

The dielectric permittivity can be measured by measuring the capacitance with the dielectric material and the capacitance in vacuum without the dielectric material.

The capacitor component with the dielectric medium is equivalently viewed as a pure capacitor in parallel with a conductor, as depicted in Figure 1,

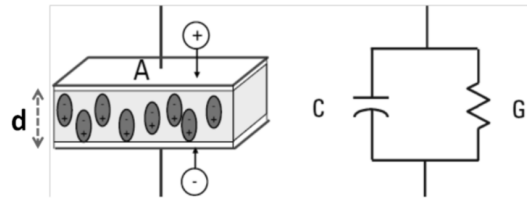


Figure 1 a parallel plate capacitor with the dielectric medium (left) and its equivalent electrical model (right)

The equivalent electric circuit model of a capacitor is usually expressed as a capacitance C in parallel with a conductance G . The admittance Y , defined as the inverse of the impedance, is usually used to describe the circuit, i.e., $Y = 1/Z = G + jB$, where G is conductance (Siemens) and B is susceptance (Siemens). Since $Y = j\omega C_0(\epsilon_r' - j\epsilon_r'')$, $B = \omega C_0 \epsilon_r'$ and $G = \omega C_0 \epsilon_r''$. G is related to the $\epsilon_r''(\omega)$, and B is related to the $\epsilon_r'(\omega)$. By measuring the real part and imaginary part of the impedance of the capacitor, the dielectric constant ϵ_r' and its loss ϵ_r'' can be experimentally determined.

In the dielectric materials with the ionic conduction, the measured loss usually includes both the dielectric loss and the conduction loss, i.e., $\epsilon_r''(\omega)_{eff} = \epsilon_r'' + \sigma / \epsilon_0 \omega$, where σ is the conductivity.

For most civil materials, $\epsilon_r'(\omega)$ is highly sensitive to the fraction of water content, and the effective loss $\epsilon_r''(\omega)_{eff}$ increases significantly via enhanced ionic conduction [13].

2.2 Capacitance Sensors

In our testing, in order to make the capacitance sensors easy to apply to the building materials, three types of capacitor configurations were tested. As shown in Figure 2 are a two-steel-bars capacitor (Two-Bars), an interdigitated arrays capacitor (IDA) and a transmission line type capacitor (SMT T-line tape (MDS-100-SS)). The Two-Bars capacitor can be installed into the drilled holes in the materials where the electric field between the bars interacts with the dielectric material to sense the variation of the dielectric constant. The IDA and the MDS-100-SS capacitors can be installed by tightly bonding them on the surface of the materials, where the infringing electric field formed between the electrodes senses the dielectric variation of the surrounding material.

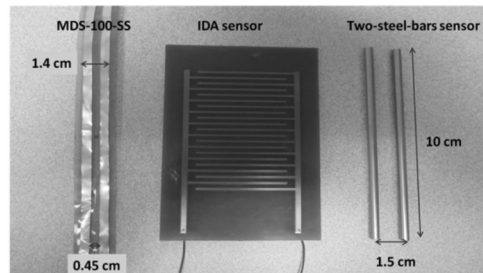


FIGURE 2: THREE TYPES OF CAPACITANCE SENSORS WITH DIFFERENT PHYSICAL CONFIGURATIONS

For the capacitors with the testing material as their dielectric mediums, the capacitance changes with the moisture content. Therefore, measurement of the capacitance can provide information of the moisture content in the materials.

2.3 Impedance Measurement Methods

There are many methods to measure impedance in terms of the measuring conditions and requirements. Selection of measurement techniques depends on the measuring frequency coverage, impedance range, accuracy and easiness of operation. The following methods: such as, Auto balancing bridge, I-V technique, RF I-V technique and Network Analyzer are often used, as described in the manual of the Agilent Impedance Analyzer. The auto balancing bridge covers the widest frequency and impedance range with high accuracy and easy operation (0-110 MHz; 1m Ω -100 M Ω); The I-V technique is good in the mid-frequency and impedance rang (10-100 MHz, 0.1 - 1 M Ω), RF I-V method has a best measurement capability for high frequency measurement (1 MHz-1 GHz; 0.1-100 k Ω), and Network Analyzer is recommended for much higher frequency range (100 kHz- above 100 GHz) with the impedance range of around 50 Ohms. These techniques have their own advantages and disadvantages depending on the specific measuring conditions.

2.4 SMT Wireless Data Logger

The SMT capacitance sensor was made using the printed circuit board technology [14]. The capacitance sensor is of the IDA configuration as shown in Figure 4. On the same PCB board, a capacitance sensing circuit was built with the PCI18f25J11 microcontroller (Microchip). The microcontroller uses the Charge Time Measurement Unit (CTMU) in conjunction with the A/D Converter to measure time and capacitance. The specific operation theory of capacitance measurement is referred to the PCI18f25J11 data sheet [15]. As shown in Figure 4, the SMT Data Acquisition Unit SMT-A2 can read the voltage on the two external ports that are connected to the output of the sensing circuit board. In the Unit SMT-A2 a wireless transmitter circuit was built to transmit the measured data wirelessly to a host computer that has SMT-I2 (802.15.4 to USB) interface.

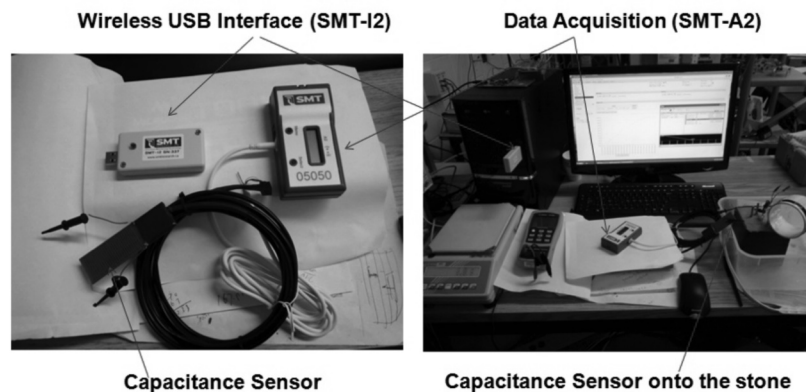


FIGURE 4: THE SMT WIRELESS DATA LOGGER (LEFT) AND THE TESTING SETUP (RIGHT)

2.5 Wireless LC Resonator Method

The electrical resonance circuit is also a method to measure the impedance. At the resonant frequency, the circuit displays the pure resistive behaviour since the capacitive and inductive impedances cancelled each other. Figure 5 shows a basic electrical LCR resonant circuit, which is constructed by connecting three electrical elements, inductance (L), capacitance (C) and resistance (R) in parallel. The resonant frequency

is defined as the frequency at which the impedance of the parallel LCR circuit becomes maximum, which is simply represented by the following mathematical equation:

$$F_r = \frac{1}{2\pi \sqrt{LC}} \quad (2)$$

Where F_r is determined by the inductance L and the capacitance C .

As widely used in building electrical oscillators and filters, this resonant characteristic also provides a way to build a sensing device, i.e., by measuring the resonant frequency, the capacitance C can be measured. Therefore, the capacitive sensing is available by monitoring the resonant frequency shift. This is the basic operating mechanism of the LC resonant sensors.

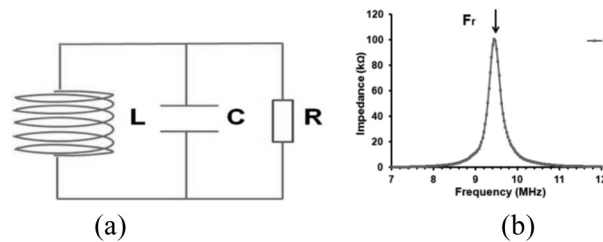


FIGURE 5: (A) A BASIC PARALLEL LCR RESONANT CIRCUIT. (B) FREQUENCY DEPENDENT IMPEDANCE DISPLAYS A RESONANT BEHAVIOUR AT THE FREQUENCY OF F_r .

The LC resonant sensor can measure the capacitance change by measuring the resonant frequency change, thus, it also can measure the water content inside the dielectric materials. The advantage using the resonant frequency measurement is that the resonant signal from the sensing component can be wirelessly detected using an interrogate antenna.

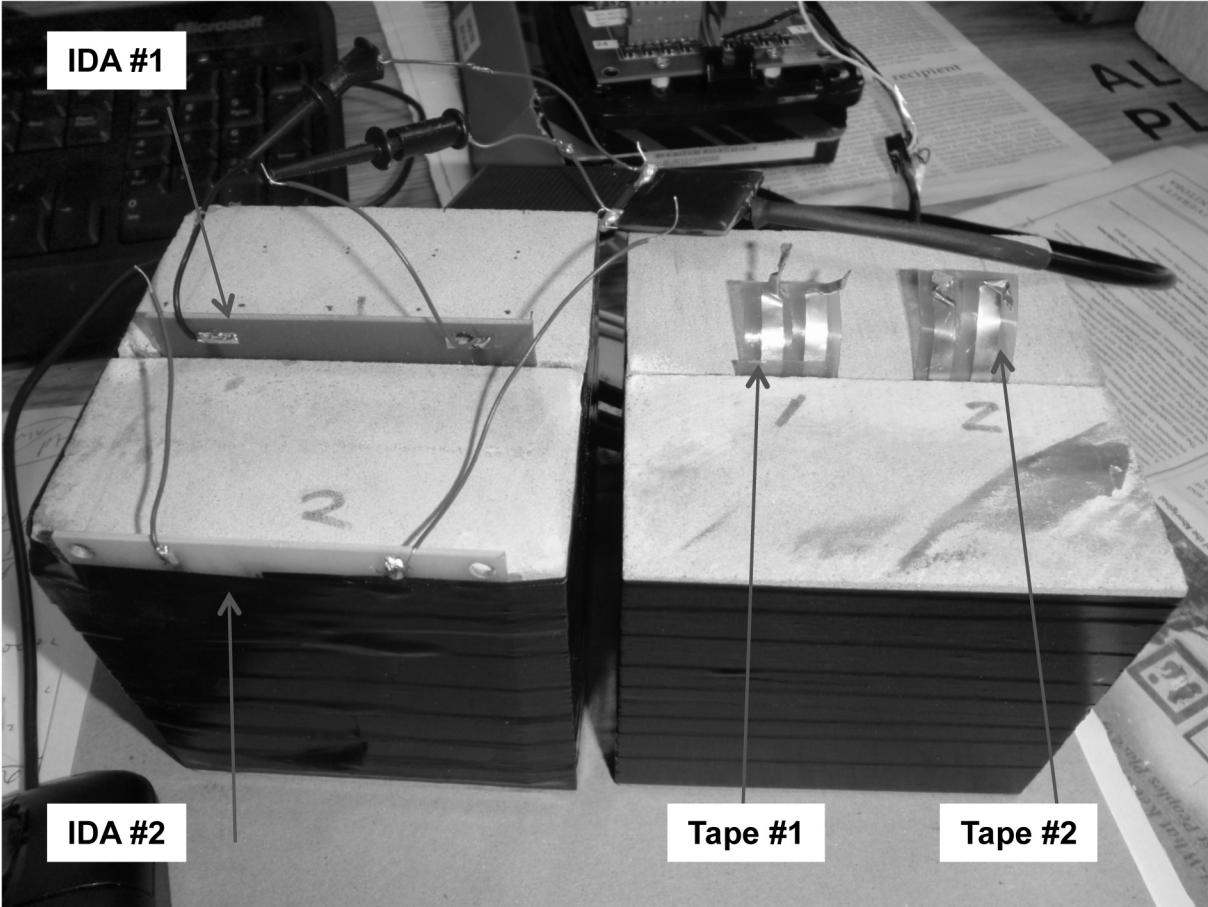
When the two-bar capacitor starts to sense the moisture, the capacitance increases significantly, this is caused by the higher dielectric constant of water. The capacitance change results in a decrease in the sensor's resonant frequency. In addition, the electrically more conductive water/stone mixture also increases the energy loss of the capacitor, leading to the reduction in amplitude of the inductively coupled signal. In the test setup, only the capacitance of the two-bars changes with the water level inside the stone while the inductance of the sensing coil remains constant. Therefore, the variation of the resonant frequency of the sensor is a direct reflection of the water content in the stone.

3 TESTING RESULTS

3.2 Testing the IDA and the SMT T-line Tape Sensors

In the following test, the two IDA sensors and two SMT T-line tape sensors were used. As shown in Figure 12, the IDA #1 sensor has electrodes with painting on it and the IDA #2 sensor has no painting on the electrodes. The tape sensor #1 has two parallel conducting electrodes which is sealed within the two folded plastic tapes. The Tape #2 sensor has two parallel electrodes exposed in one side of the tape. The IDA #1 sensor was sandwiched between two pieces of stones and IDA #2 was tightly bonded on the side wall of the stone with the conducting electrodes directly in contact with the stone surface. Tape #1 sensor and tape #2 sensor were sandwiched between two pieces of the stones, the electrodes of tape #1 was not in direct contact with the surface of the stone, hence it is electrically DC-blocked since the electrodes are sandwiched between the plastic tapes. The Tape #2 electrodes are exposed and are in direct contact with the surface of the stone.

Two short wires with the small clips are used to connect the testing sensors to the SMT IDA sensor in parallel. Their total capacitance is read by the on-board PIC capacitance controller and the data is sent to the data logger. The data logger wirelessly sends the captured data to the computer.



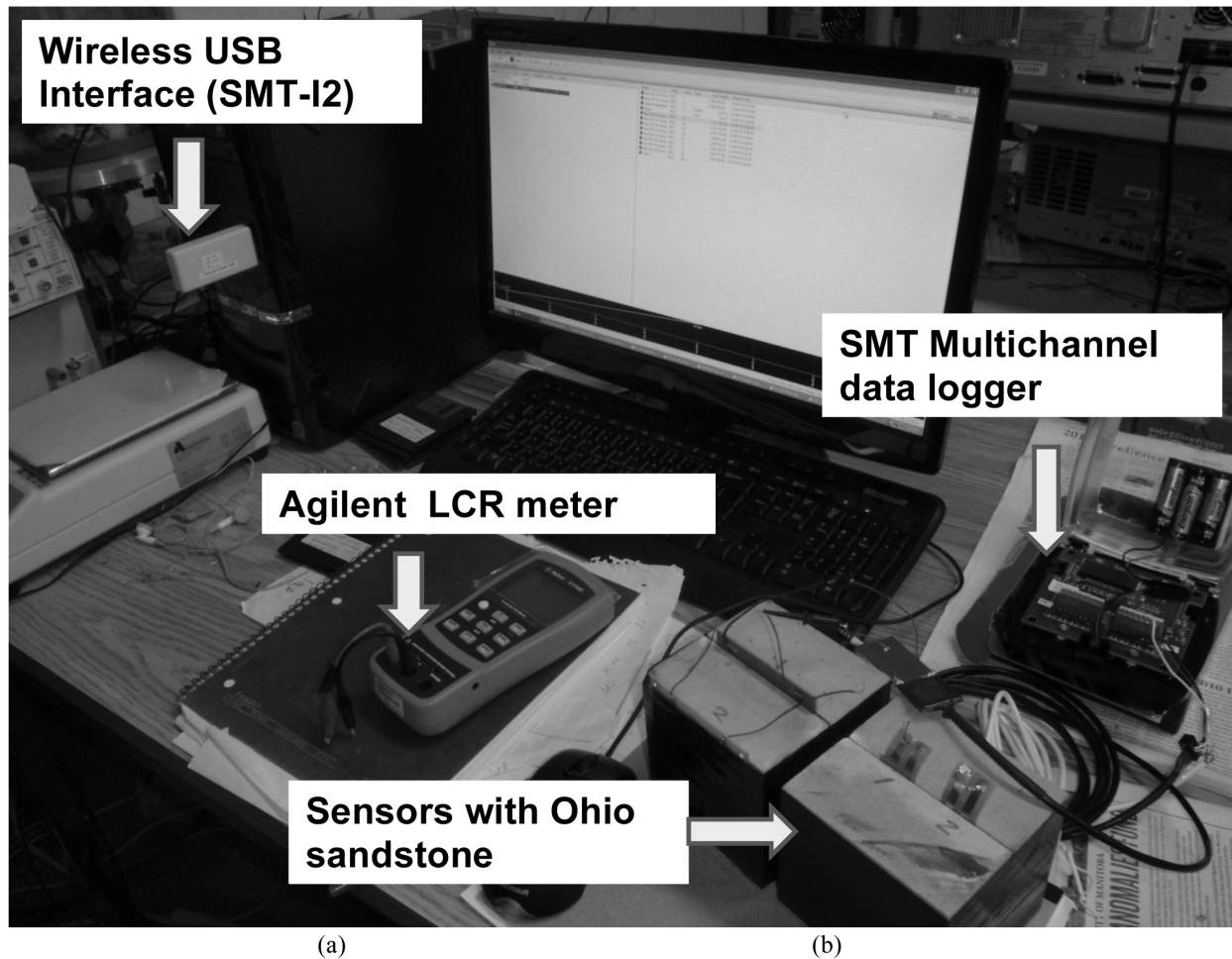


FIGURE 12: THE INSTRUMENTED STONES WITH CAPACITANCE SENSORS AS IN (A) AND THE TESTING SET UP AS IN (B).

The testing was carried out by first putting the instrumented stones inside a water container. The water was absorbed from the bottom of the stone then transported upward to the top surface of the stone until the stone was totally wetted (moisture saturated). The measurement data was only taken for the lab dry state and the saturated state during the wet in this testing since the detailed wetting process was described in the previous section. After the stones were moisture saturated, the continuous measurement was done during the drying of the instrumented stones. The drying was only through the bottom and top side of the stone since the side walls of the stones were moisture insulated using the moisture barrier tape.

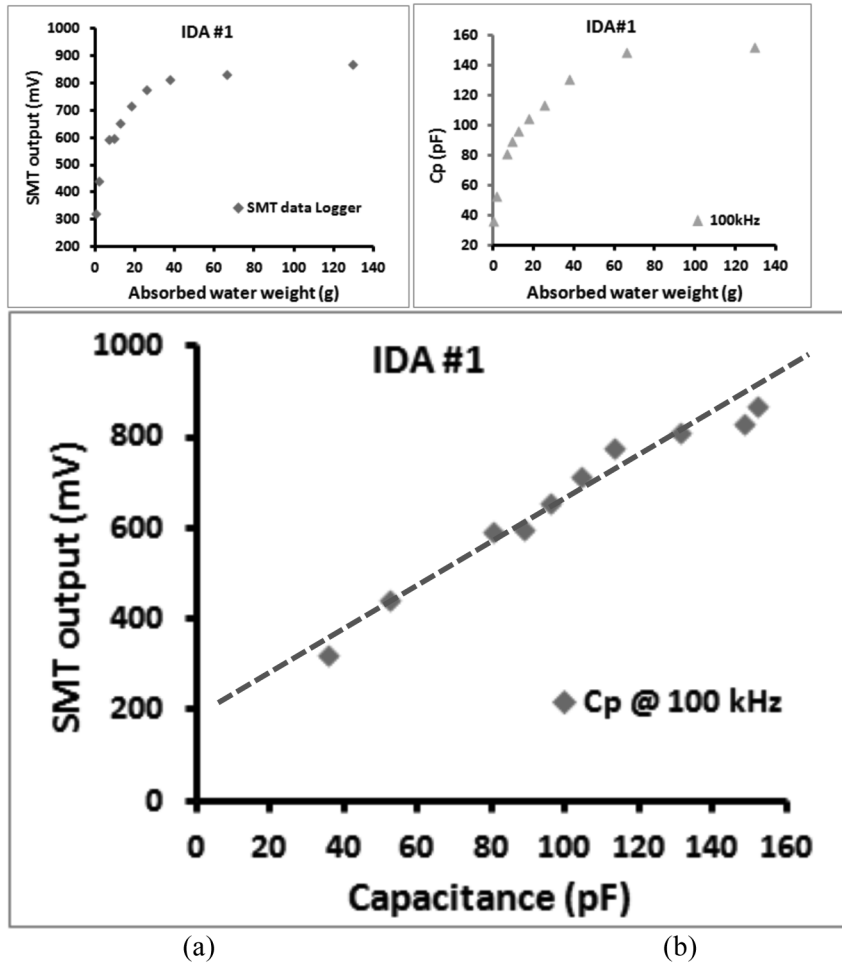


FIGURE 13: THE SMT OUTPUT VERSUS THE ABSORBED WATER WEIGHT DURING DRYING IN (A), THE CAPACITANCE VERSUS ABSORBED WATER WEIGHT IN (B) AND THE CORRELATION BETWEEN A AND B IS SHOWN IN (C).

Figure 13 show the data measured for the IDA #1 sensor. Figure 13 (a) shows the SMT output versus the absorbed water weight for the instrumented stone, Figure 13(b) shows the capacitance measured using the LCR meter at the frequency of 100 kHz, and Figure 13 (c) is the SMT output versus the capacitance. The data were measured during the drying. The drying always started from the top and bottom surface and that is why the large weight reduction during the first two days is not quickly responded by the sensor, the capacitance and the output of the SMT data logger did not reduce that much corresponding to the large reduction in the moisture weight because the moisture condition surrounding the electrodes was still close to the saturated state. The moisture state surrounding the sensor electrodes is a dominant factor on the capacitance rather than the moisture state far away from the electrodes.

3.3 Capacitance and Resonant Frequency Variation in a Wet-Dry Cycle

Figure 17 shows capacitance change versus the absorbed moisture content in the wetting and drying process for the IDA#1 type sensor, in Figure 17 (a) the capacitance measured with different frequencies during the drying shows the capacitance dependence on the measuring frequency. In Figure 17 (b) the capacitance change in a wet-dry cycle shows a hysteresis behaviour, it suggests that correspondence of the capacitance

change to the moisture absorption and evaporation is different due to that the moisture sensing by the electric field undergoes the different moisture transport behaviour and paths.

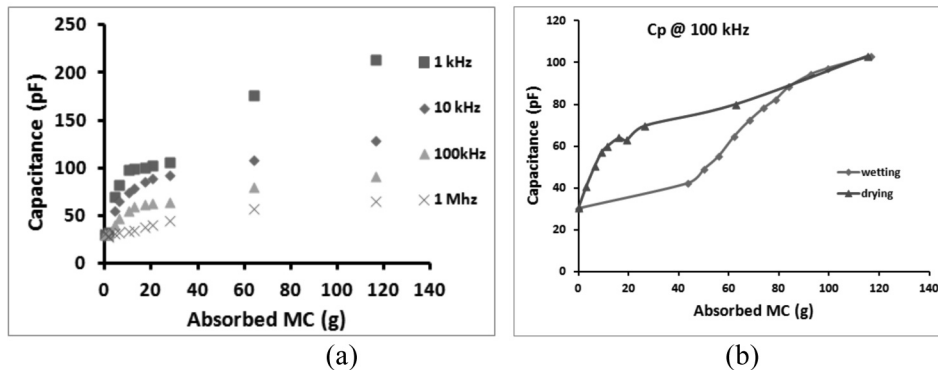


FIGURE 17: (A) IS THE CAPACITANCE MEASURED AT DIFFERENT FREQUENCIES VERSUS THE ABSORBED MOISTURE CONTENT AND (B) IS HOW THE CAPACITANCE VARIES DURING THE WETTING AND THE DRYING.

Figure 18 shows the data measured using the LC resonant sensor, in this testing the capacitance sensor is the IDA sensor, the LC resonant sensor is composed of the IDA capacitor and the inductive coil inductor in parallel. In Figure 18 (a) shows the measured data of the resonant frequency and quality factor of the LC resonant sensor for the two moisture states: the dry state with the MC of 0 g and the wet state with the MC of 116 g. The resonant frequency shifted from 3.504774 MHz in the dry state down to the 2.579967 MHz in the wet state while the quality factor dropped from 63 to 4.4. Figure 18 (b) shows the resonant signal acquired through the interrogator coil with the impedance analyzer.

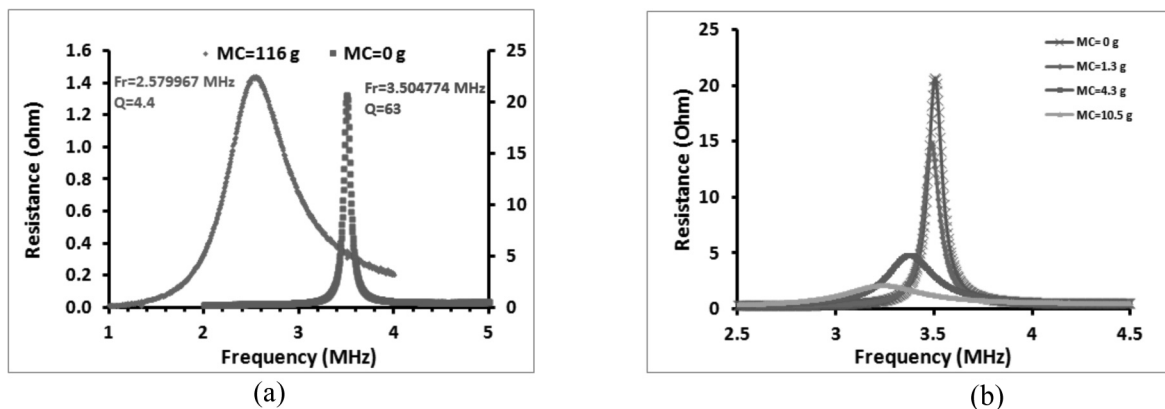


FIGURE 18: IN (A) THE RESONANT FREQUENCIES AT THE TWO PEAKS CORRESPOND TO THE DRY STATE (MC=0 G) AND WET STATE (MC=116 G) OF THE STONE, (B) SHOWS HOW RESONANT SIGNAL CHANGES WITH MOISTURE CONTENT

4. Results for Three Types of Stones using Two-Steel-Bars Capacitance Sensor

Three types of masonry stone blocks commonly used on Parliament Hill: St. Canut sandstone, Ohio sandstone and Limestone, were cut into 100 mm cubic specimens. A hole with a diameter of 10 mm and a depth of 40 mm was drilled in the center of the stone facet for housing relative humidity (RH) sensor. The

RH sensors were fixed into PVC tubes and embedded into the drilled holes which then were sealed using instant epoxy. Another four holes with a diameter of 5 mm and depth of 40 mm were drilled for mounting stainless steel bars as electrical electrodes. Stainless steel bars with a diameter of 4.5 mm and a length of 70 mm were mounted inside the holes using conducting silver epoxy. Two steel bars are used for electrical resistance and capacitance measurement. Another two steel bars, acting as a capacitor (a two-parallel-bar capacitor), are connected to an inductive coil to form an inductance-capacitance (LC) resonant electrical circuit which behaves as a resonant frequency sensing device. The side walls of stone specimens were wrapped using a moisture barrier tape. The prepared stone specimens are shown in Figure 19.

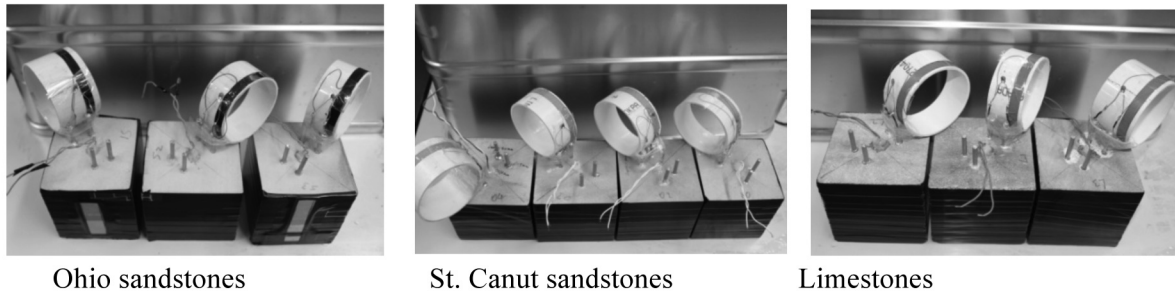


FIGURE 19: THE PREPARED STONE SPECIMENS WRAPPED WITH A MOISTURE INSULATING TAPE HAVE THE RELATIVE HUMIDITY (RH) SENSORS MOUNTED IN THE HOLES LOCATED IN THE CENTER OF THE UPPER SIDE OF THE STONES; THE TWO STAINLESS STEEL BARS AS ELECTRODES AND THE INDUCTANCE-CAPACITANCE (LC) RESONANT SENSORS COMPOSED OF AN INDUCTIVE COIL AND A TWO-PARALLEL-BAR CAPACITOR.

The monitoring of moisture content in the sandstone specimens was carried out by measuring the instrumented specimen weight, electrical resistance, capacitance and resonant frequency shift during the wetting and drying cycle. The stones underwent the wetting cycle by being placed into deionized (DI) water of about 2 mm high. Once the stones were saturated, the drying cycle took place in the lab environment after the stones were taken out of the water. It is important to note that only the bottom side of the stone is in contact with the DI water. The absorbed moisture can only travel upward because the side walls of the stones are wrapped with moisture insulated tape. Thus, the moisture transport in the stones can be viewed as a one-dimensional moisture transport problem. This is also similar to the real physical process where one side of a stone wall is exposed to the external environment and the opposite side faces the inside of the building.

4.1 Relative Humidity (RH) Moisture Measurement

The relative humidity (RH), the DC resistance (DC-R) and capacitance (C) of the two steel bars were measured during the wetting and the drying cycles while the moisture weight variation with time was also measured. For each specimen from the three types of the stones, the measured RH and DC-R were plotted against the moisture weight percentage relative to their stone weights in the dry state. Figure 20 shows the RH versus percent of maximum weight of water absorbed during test for three specimens, where the water content was normalized to the maximum water content as listed in Table 2. The data clearly indicates that a very small amount of the water content (<2% for sandstones, <15% for limestone) will saturate the RH sensor. This result suggests the RH sensor is not an appropriate way to measure the water content inside the stone specimens.

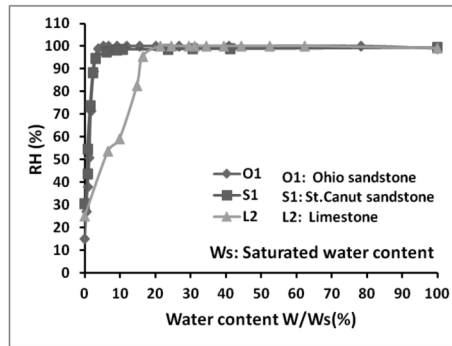


FIGURE 20: RH VERSUS PERCENTAGES OF ABSORBED MOISTURE CONTENTS TO THEIR RESPECTIVE MAXIMUM WEIGHTS

4.2 DC-Resistance versus Moisture Content

Figure 21 presents the measured DC-R values for three specimens O3, S2 and L2 during the drying process. The data is plotted in a log-log format to easily display all the data in one diagram. The data indicates that the DC-R values vary largely between the wet and dry state, ranging from around a hundred k Ω to a value much larger than the 120 M Ω measurement limitation of the multimeter. In reality, the DC resistance can be up in the range of G Ω for the dry stones. In this test, for the wet state for three types of the stones, the Ohio stone O3 has the DC resistance of about 80 k Ω , the limestone L2 shows resistance value around 200 k Ω and the St. Canut sandstone S2 has a resistance of about a few M Ω . By comparing the absorbed moisture weight for St. Canut stone to that for lime stone, the measured DC resistances for these two types of stones suggests the St. Canut stone has a much lower conductivity than the limestone even the former absorbed more water than the latter. When measuring the DC-R, the existence of polarity effect was observed and the resistance value shows a difference when the polarity of the two electrodes was switched. Also, the resistance changes with the measuring duration time, revealing a strong influence of the charged ions accumulation process surrounding the two electrodes [17, 18]. The measurements using 2-probe and 4-probe methods in this testing did not show a significant difference because of the large resistance relative to the contact resistance. The relationship between the resistance and the moisture content is very specimen-dependent. This reflects the difference in the mineralogical compositions and the microstructure of the stones, leading to the difference in the ionic conduction.

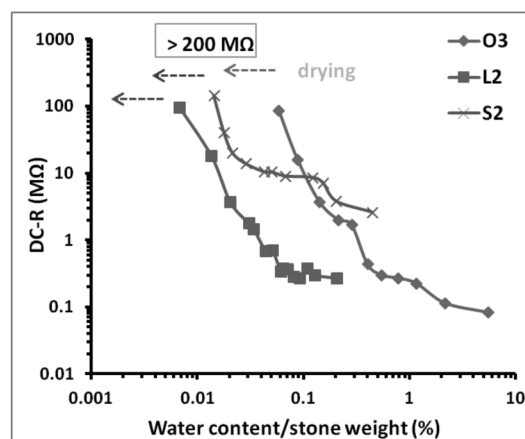


FIGURE 20: DC-RESISTANCES VERSUS PERCENTAGE OF ABSORBED MOISTURE CONTENTS TO THEIR RESPECTIVE STONE WEIGHTS

4.3 Capacitance and Conductance at Frequency of 1 MHz

The capacitance (C_p) and conductance (G) of the two steel bars inside the specimens were measured with frequency sweep range from 1 MHz to 10 MHz during the wetting and the drying process. Table 4 shows the capacitance C_0 and the conductance G_0 at a frequency of 1 MHz which was measured before the wetting and drying cycle. The capacitances for all specimens increased with moisture content as expected. For the Ohio sandstone, with a moisture content increase up to about 5% (relative to the drying state in the lab environment), the normalized capacitances increased about 2.0-2.2 times. For the limestone, the normalized capacitance increased 1.3-1.5 times for a 0.1% increase in moisture content. For the St. Canut sandstone, the normalized capacitance increased only about 1.0-1.15 times corresponding to the moisture content increase of about 0.4-0.5%. In addition to the capacitance at frequency of 1 MHz, the conductance (G) can also provide useful information related to the moisture content in three types of specimens. For the Ohio sandstones, the normalized conductance increased about 200 times (from about $1\mu\text{S}$ to $200\mu\text{S}$) with an increase of the water content of about 5%. It is interesting to note that the conductance (G) behaves linearly with the water content. The data for these three specimens are very close and also display a good linear behaviour. This linear relationship between the conductance and the water content suggests a new way for constructing moisture sensors in terms of conductance variation with moisture content.

4.4 Resonant Frequency and Capacitance Versus Moisture Content

Resonant frequency (F_r) shift and capacitance variation at the resonant frequencies during the wetting and drying cycles were measured for three specimens of each type of stone. Resonant frequency, capacitance and moisture weight against time were recorded. For the Ohio sandstones, data points of the normalized resonant frequencies for the three specimens agree well with each other. The resonant frequency in the wet state dropped down to about 0.94 of the resonant frequency F_0 in the dry state. Meanwhile, the normalized capacitances, corresponding to the resonant frequencies, increased up to 1.4-1.5 times, and also show good data convergence at the lower percentage of water content. Similarly, the data for three limestone specimens show the resonant frequency shifted down to the 0.94 of the F_{r0} while the capacitance changed to about 1.2 of the C_0 at the water weight percentage of about 0.1%. This is much smaller than the water percentage for those Ohio sandstone specimens, confirming the difference in the moisture transport and storage between the sandstones and the limestones under testing.

The resonant frequency measurement data clearly demonstrates that the resonant frequency shift is well correlated with the dielectric permittivity change that is induced by the changing moisture content inside the stones. By measuring the resonant frequency, the moisture content can thus be monitored once the calibration curve for the stone is made. In comparison with the RH data described above, the resonant frequency sensing technique provides a consistent correlation with the moisture content with a wide sensing range without saturation problem as encountered in the RH sensing.

The above testing results lead to the following conclusions:

- 1) The RH sensor is not a good indicator of liquid water in stone. In this test, the RH sensor only works at the very low moisture level less than 10% of the maximum absorbed water.
- 2) The electrical resistance of the stones does change monotonically with moisture content. However, measurement is limited by instrument range. In this test, the resistance changes very fast with the moisture content, ranging from the values much larger than a few hundred $\text{M}\Omega$ (up to $\text{G}\Omega$) in a dry state down to the magnitudes less than a few hundred $\text{k}\Omega$. The resistance also varies very differently from specimen to

specimen, suggesting the existence of a variety of conducting ions and the ionic electrical conduction.

3) The capacitance changes with the moisture content inside the stones, as expected, during the wetting and the drying cycles. As observed in the test, direct capacitance measurement is affected with the wire configuration and the surrounding environment between the specimen and the capacitance instrument. However, with sufficient care repeatable water content measurements can be made.

4) The resonant frequency measurements show consistent variation responding to the change of the moisture content during the wetting and the drying cycles. Specifically, the LC resonant frequency change responds very well to the change of the moisture content. The LC resonant frequency measurement can be accomplished wirelessly without direct wire connection between the instruments and the specimens.

5 SUMMARY

In summary, the dielectric (capacitive) method of estimating the moisture content (MC) in the masonry stones is effective and practical; it is useful to measure the MC over the dry to the moisture saturated state. The MC measurement can be accomplished using either the direct capacitive sensing or the passive wireless inductor-capacitor (LC) resonant frequency sensing. The capacitance sensing can be done using the LCR handheld meter or capacitance microcontroller with integrated wireless data logger. In this testing three types of capacitance sensing components were investigated for detecting the moisture content in the building stones. The testing results demonstrate that the capacitance sensors and the data loggers are capable of measuring the moisture content in the building stones. Further measurement calibration and field deployment of these techniques are expected to lead to practical applications in the field of structural health monitoring.

REFERENCES

- [1] Farrar C R and Worden K A(2007) *An introduction to structural health monitoring Phil. Trans. R. Soc.* 365, 303–315
- [2] Lynch J P A(2007) *An overview of wireless structural health monitoring for civil structures Phil. Trans. R. Soc.* 365, 345–372
- [3] Mufti A A 2003 *Integration of Sensing in Civil Structures: Development of the New Discipline of Civionics, Proceedings for the First International Conference on Structural Health Monitoring and Intelligent Infrastructure (SHMII-1 2003)*
- [4] Rivera E, Mufti A A and Thomson D J 2007 *Civionics for structural health monitoring Can. J. Civ. Eng.* 34: 430–437
- [5] Tada S and Watanabe K 1998 *An Overview of Principles and Techniques of Moisture Properties Measurement for Building Materials and Components, France-Japan Workshop on Mass Energy Transfer and Deterioration of Building Materials and Components, 22-23, Tsukuba, Japan*
- [6] Nady M and Saïd A 2007 *Measurement Methods of Moisture in Building Envelopes - A Literature Review International Journal of Architectural Heritage, 1: 3, 293-310*
- [7] Ong J B, You Z, Mills-Beale J, Tan E L, Pereles B D and Ong K G 2008 *IEEE sensors*, 8, 2053
- [8] Bhadra S, Bridges G E and Thomson D J 2010 *Coupled Coil Sensor for Detecting Surface Corrosion on Steel Reinforcement, 14th International Symposium on Antenna Technology and Applied Electromagnetics [ANTEM] and the American Electromagnetics Conference [AMEREM]*

- [9] Ruhanen A, Hanhikorpi M, Bertuccelli F, Colonna A, Malik W, Ranasinghe D, López T S, Yan N, Tavilampi M 2008 *Sensor-enabled RFID tag handbook, BRIDGE – Building Radio Frequency Identification Solutions for the Global Environment*
- [10] Sidén J, Zeng X, Unander T, Koptyug A and Nilsson H E 2007 *Remote Moisture Sensing utilizing Ordinary RFID Tags IEEE SENSORS 2007 Conference* 308-311
- [11] Kim S, Pakza S, Culle D, Demmel J, Fenve G, Glaser S, Turon M 2007 *Health Monitoring of Civil Infrastructures Using Wireless Sensor Networks IPSN'07*
- [12] Büyükköztürk O, Yu T Y, Ortega J A 2006 *A methodology for determining complex permittivity of construction materials based on transmission-only coherent, wide-bandwidth free-space measurements, Cement & Concrete Composites* 28, 349–359
- [13] Rusiniak L 1998 *Dielectric Constant of Water in a Porous Rock Medium, Phys. Chem. Earth*, 23, 1133-1139
- [14] Dean R N, Rane A, Baginski M, Richard J, Hartzog Z and Elton D J 2012 *A capacitive fringing field sensor design for moisture measurement based on printed circuit board technology, IEEE Trans. on Instrumentation and Measurement*, 61, pp. 1105-1112.
- [15] 2011 *Microchip Technology Inc. PIC18F46J11 Family Data Sheet.*
- [16] Finkenzeller K 2003 *RFID Handbook: Fundamentals and Applications in Contactless Smart Cards and Identification, Wiley*
- [17] Gomaa M M 2008 *Relation between electric properties and water saturation for hematitic sandstone with frequency, Analysis of Geophysics*, 51
- [18] Liu Y, Tang J, Mao Z 2009 *Analysis of bread loss factor using modified Debye equations Journal of Food Engineering* 93, 453–459